Aggregates of Acetylcholine Receptors Are Associated with Plaques of a Basal Lamina Heparan Sulfate Proteoglycan on the Surface of Skeletal Muscle Fibers

M. JOHN ANDERSON and DOUGLAS M. FAMBROUGH

Carnegie Institution of Washington, Department of Embryology, Baltimore, Maryland 21210. Dr. Anderson's present address is Department of Pharmacology and Therapeutics, University of Calgary, School of Medicine, Calgary, Alberta, Canada T2N 1N4.

ABSTRACT Hybridoma techniques have been used to generate monoclonal antibodies to an antigen concentrated in the basal lamina at the *Xenopus laevis* neuromuscular junction. The antibodies selectively precipitate a high molecular weight heparan sulfate proteoglycan from conditioned medium of muscle cultures grown in the presence of [^{35}S]methionine or [^{35}S]-sulfate. Electron microscope autoradiography of adult *X. laevis* muscle fibers exposed to ^{125}I-labeled antibody confirms that the antigen is localized within the basal lamina of skeletal muscle fibers and is concentrated at least fivefold within the specialized basal lamina at the neuromuscular junction. Fluorescence immunocytochemical experiments suggest that a similar proteoglycan is also present in other basement membranes, including those associated with blood vessels, myelinated axons, nerve sheath, and notochord.

During development in culture, the surface of embryonic muscle cells displays a conspicuously non-uniform distribution of this basal lamina proteoglycan, consisting of large areas with a low antigen site-density and a variety of discrete plaques and fibrils. Clusters of acetylcholine receptors that form on muscle cells cultured without nerve are invariably associated with adjacent, congruent plaques containing basal lamina proteoglycan. This is also true for clusters of junctional receptors formed during synaptogenesis in vitro. This correlation indicates that the spatial organization of receptor and proteoglycan is coordinately regulated, and suggests that interactions between these two species may contribute to the localization of acetylcholine receptors at the neuromuscular junction.

The vertebrate neuromuscular junction is a region of elaborate morphological specialization for both the skeletal muscle fiber and motor neuron. This morphological complexity reflects a corresponding chemical specialization. It is well established, for example, that the postsynaptic membrane of the muscle fiber contains a high concentration of acetylcholine receptors (AChR),[1] and that the packing density of this integral membrane protein drops at least 50-fold within a few micrometers of the nerve terminal (1). It is also known that acetylcholinesterase (AChE) is concentrated within the synaptic cleft (2, 3), where it appears to be associated with the basal lamina (4, 5). Immunocytochemical experiments indicate the existence of further chemical specialization in the muscle cytoskeleton (6–8), basal lamina (9), and the nerve terminal (10, 11). Undoubtedly the list of components concentrated at the neuromuscular junction will continue to increase as improved immunological techniques permit the identification and study of new molecular entities.

In contrast to such evidence for chemical specialization, little is known about the cellular mechanisms responsible for the elaboration of the neuromuscular junction during development. It has been shown, however, that developing cholinergic nerve fibers can induce the formation of new aggregates of AChR during the establishment of neuromuscular junctions on embryonic muscle cells in culture (12–14) and at

[1] *Abbreviations used in this paper:* AChE, acetylcholinesterase; AChR, acetylcholine receptor; αBGT, α-bungarotoxin; FITC, fluorescein isothiocyanate; and TRITC, tetramethylrhodamine isothiocyanate.

THE JOURNAL OF CELL BIOLOGY · VOLUME 97 NOVEMBER 1983 1396–1411

ectopic sites on denervated adult muscle (15). These observations suggest that the regional chemical specialization that occurs during synaptogenesis results in part from a reorganization of plasma membrane proteins that is dependent upon a localized inductive interaction between nerve and muscle. This interpretation is complicated by observations that analogous aggregates of AChR also develop in aneural muscle cultures (16, 17), upon denervated adult muscle fibers (18), and in adult muscle regenerating within sheaths of extracellular matrix (19). Such evidence indicates that the clustering of AChR, whether at the developing neuromuscular junction or in the absence of nerve, is secondary to unknown events associated with muscle development and innervation.

In both denervated and innervated muscle fibers, AChR occur in two organizational states: a dispersed, mobile phase and densely packed immobile clusters (20). One explanation of this distribution is that some AChR become immobilized due to adhesive interactions either with one another or with immobile structural proteins, such as might be found in the adjacent cytoskeleton or extracellular matrix. Immunocytochemical experiments have in fact suggested the existence of appropriate specializations of cytoskeletal and extracellular matrix elements at the neuromuscular junction (6–9), but limitations of the available antibody preparations have so far precluded a rigorous identification (however, see reference 8). In our study, we used hybridoma techniques (21) to identify and characterize a heparan sulfate proteoglycan that shows a notable concentration in the basal lamina at the neuromuscular junction, and whose surface organization is also remarkably homologous with AChR clusters found on both innervated and aneural muscle cells developing in culture.

MATERIALS AND METHODS

Preparation of Monoclonal Antibodies: We immunized BALB/cJ mice by intraperitoneal injection of insoluble material from *Xenopus laevis* larval tails that had been homogenized, washed, and resuspended in complete Freunds' adjuvant. After 4 wk the mice were again injected with the same immunogen without adjuvant. 3 d later the mice were killed by cervical dislocation and their spleens removed under sterile conditions. Lymphocytes were isolated from these spleens and fused with SP2/0 myeloma cells essentially as described by Kennett et al. (22). Conditioned culture medium from the hybridoma cultures was harvested and assayed for binding to cryotome sections of *X. laevis* larval tail muscle by indirect immunofluorescence using fluorescein conjugated goat anti-mouse IgG (Cappel Laboratories, Cochranville, PA). Before sectioning, the larval muscle had been counterstained with tetramethylrhodamine-conjugated α-bungarotoxin (αBGT) (23) to reveal synaptic sites. Hybridoma cultures producing antibody to *Xenopus* antigens were cloned in soft agar and propagated as ascites tumors in BALB/cJ mice. The isotype of the monoclonal immunoglobulins was determined by metabolically labeling the hybridoma secretory products with [^{35}S]methionine, and analyzing their composition by electrophoresis in SDS-containing polyacrylamide gels (24), followed by fluorography (25, 26). In the cases reported here the labeled antibodies consisted only of heavy and light chains characteristic of IgG. Based upon this analysis, monoclonal antibodies were isolated from pooled ascitic fluid by ammonium sulfate fractionation followed by ion-exchange chromatography on DEAE-cellulose.

Preparation of Dye-conjugated Monoclonal Antibody: Solutions of monoclonal IgG were adjusted to pH 9.5 by the addition of one-tenth volume 1 M Na_2CO_3 which had been adjusted to pH 9.5 with HCl. Fluorescein isothiocyanate (FITC) (Molecular Probes, Inc., Junction City, OR) or tetramethylrhodamine isothiocyanate (TRITC) (Research Organics, Inc., Cleveland, OH) was dissolved in 0.1 M carbonate buffer pH 9.5 at 0°C. Five aliquots of dye at 12 μg FITC/mg IgG or 18 μg TRITC/mg IgG were added at 30-min intervals to the antibody with constant stirring at room temperature (22–24°C). 3 h after the first addition the reaction mixture was concentrated to ~1 ml in a B15 Minicon cell (Amicon Corp., Danvers, MA) and labeled antibody isolated by gel filtration on Biogel-P2 (Bio-Rad Laboratories, Richmond, CA). Dye-to-protein molar ratios were estimated from the ratio of absorbance at 280 nm to that at 495 or 546 nm (for FITC or TRITC, respectively) and consisted approximately of 8–10 mol FITC/mol IgG, or 2–3 mol TRITC/mol IgG. Dye conjugates were divided into 1–5-ml aliquots and stored at −70°C until use.

Primary Cultures of X. laevis Embryos: Detailed procedures for the preparation of primary cultures of *X. laevis* myotomal muscle cells, with or without neural tissues, have been described previously (13). Briefly, small pieces of embryonic stage 24–26 (27), myotomal tail muscle were isolated by sterile dissection with fine needles in the presence of ~1 mg/ml collagenase (type I, Worthington Biochemical Corp., Freehold, NJ). After dissociation in trypsin-EDTA, cells were plated on collagen-coated glass coverslips (or collagen-coated plastic culture dishes) in 70% vol/vol HEPES-buffered Dulbecco's modified Eagles medium (DME; Gibco Laboratories, Grand Island, NY) supplemented with 1–5% vol/vol fetal bovine serum. After plating at room temperature for approximately a day to allow cell attachment to the substrate, cultures could be maintained at 10°C for up to a month before use.

When cultures were to be used for metabolic labeling with radioactive precursors, cells were plated at high density with minimal removal of connective tissue rudiments. Such cultures consisted of striated muscle cells separated by a confluent cell sheet containing a variety of fibroblastic and epithelial cells. Cultures used for fluorescent staining were plated at substantially lower densities (one to two embryos per dish), contained few connective tissue cells, and were devoid of visible neurons.

Preparation of Metabolically Labeled Secretory Products: Confluent cultures containing *Xenopus* muscle and connective tissue cells (see above) were labeled with 100 μCi/ml [^{35}S]methionine (1,100 Ci/mmol; Amersham, Arlington Heights, IL) or 400 μCi/ml [^{35}S]sodium sulfate (0.9 Ci/mmol) dissolved in carrier-free 70% vol/vol MEM supplemented with 1–2% fetal calf serum. During labeling we maintained cultures in 5% CO_2 at room temperature for 1–3 d. Medium conditioned for 2 d proved to be most suitable in that substantial labeling was combined with less proteolytic degradation of secreted proteins than occurred at longer incubation periods.

After exposure to cells, the labeled medium was removed, pooled, routinely diluted 1:1 with borate-buffered saline, pH 7.8 containing 2 mM phenylmethanesulfonylfluoride, 5 mM *N*-ethylmaleimide, and 5 mM EDTA to limit subsequent proteolytic degradation, and centrifuged for 20 min at 20,000 *g* at 4°C to remove cellular debris.

In some experiments, where glycosaminoglycan lyase degradation was to be carried out directly on the conditioned medium, the addition of protease inhibitors and borate-buffered saline was omitted.

Immune Precipitation of Labeled Antigens: The ^{35}S-labeled secreted antigen was purified from the diluted conditioned medium (see above) by adding 10 μg of monoclonal mouse IgG to 1 ml in 1.5 ml microfuge tubes. After incubation at room temperature for 1–2 h, ~40 μg of goat anti-mouse IgG were added and the mixture incubated for a further 1–2 h at room temperature, followed by overnight at 0°C. The immune precipitate containing labeled antigen was separated from the conditioned medium by sedimentation at ~1,000 *g* for 5 min in a clinical centrifuge, followed by aspiration of the supernatant. The pelleted immune precipitate was washed three to four times by resuspension in BBS and recentrifugation. The pellets were then either dissolved in SDS-containing sample buffer for electrophoresis, or exposed at 37°C to glycosaminoglycan lyases of various specificities (see below).

Enzymatic Degradation of Labeled Secretory Products: *Proteus vulgarus* chondroitinase ABC (E.C. 4.2.2.4) (28), *Flavobacterium heparinum* heparinase (E.C. 4.2.2.7) (29–31), *Pseudomonas* keratanase (keratan sulfate 4-galactopyranosyl glycanohydrolase) and *Streptomyces* hyaluronidase (E.C. 4.2.2.1) were obtained from Seikagaku Kogyo, Co. (Miles Laboratories, Elkhart, IN). An additional extract of heparinase was obtained from Dr. A. Linker, University of Utah (courtesy of Dr. G. Martin, National Institute of Dental Research). Stock solutions were prepared in 0.125 M Tris-HCl, pH 6.8, containing 10 mM $CaCl_2$, at 0.1 mg/ml heparinase and 0.2 mg/ml for all others. In some experiments immune precipitates (see above) were resuspended in 40 μl of enzyme solution and incubated for 4 h at 37°C. In other experiments ^{35}S-labeled conditioned medium from *Xenopus* cells was mixed 1:1 with the enzyme solution and incubated at 37°C for 4 h. In one case, immune precipitation (see above) was carried out from conditioned medium after such an exposure to heparinase. Reactions were stopped by the addition of concentrated sample buffer, yielding concentrations of 1% wt/vol SDS and 10% vol/vol glycerol (with or without 0.1 M mercaptoethanol) followed by incubation for 5 min at 100°C.

Analysis of ^{35}S-labeled Products by Gel Electrophoresis: Labeled proteins were separated by one-dimensional SDS PAGE carried out using the buffer systems of Laemmli and Favre (24). The rectangular slab gel consisted of a linear 3–15% wt/vol acrylamide gradient, with a bisacrylamide-monomer ratio of 1:37.5 (wt/wt). The stacking gel consisted of 3% acrylamide. To reveal the position of ^{35}S-labeled bands acrylamide gels were impregnated with either 2,5 diphenyloxazole (25, 26) or "Enhance" (New England Nuclear,

Boston, MA) before drying and fluorography at −70°C on Kodak XAR sheet film with or without prefogging. Apparent molecular weights of labeled cell products on each gel were estimated by comparison with conventional globular protein standards reduced in mercaptoethanol, including fibronectin (M_r 230,000), β-galactosidase (M_r 130,000), phosphorylase A (M_r 100,000), bovine serum albumin (M_r 68,000), pyruvate kinase (M_r 57,000), ovalbumin (M_r 43,000), and desoxyribonuclease (M_r 32,000), which were visualized by staining with Coomassie Brilliant Blue. In other experiments, ^{14}C-labeled protein standards (Bethesda Research Laboratories, Inc., Gaithersburg, MD) were used to permit direct visualization of the standards on each fluorograph. In all cases apparent molecular weights of the high molecular weight antigens were estimated by extrapolation from plots of log molecular weight against R_f (electrophoretic mobility) of the standard proteins.

Fluorescence Microscopy: Immunofluorescent stained tissue sections and cultured *Xenopus* muscle were examined with a Zeiss WL microscope equipped for incident illumination with narrow-band selective filter combinations for FITC and TRITC. The substitution of a 520–560-nm band-pass barrier filter in the FITC channel was found to be essential to prevent the artifactual cross over of intense TRITC fluorescence. Fluorescence intensity was also optimized by the use of an HBO100 lamp and high numerical aperture Zeiss Planapochromat oil-immersion phase-contrast objectives (Carl Zeiss, Inc., Thornwood, NY). Fluorescence micrographs were prepared on Ilford HP5 film developed in Microphen developer for 18 min at 20°C.

Autoradiography: Purified monoclonal IgG was iodinated by the chloramine-T method (32) yielding a specific activity of about 1.5×10^6 Ci/M. Sartorius muscles from small *X. laevis* adults were dissected into frog Ringer solution. Silk thread was used to attach each muscle at resting length to a wire frame, and the stretched muscle on its frame was placed in a 12 × 75–mm test tube containing incubation medium with 5 μg/ml ^{125}I-labeled monoclonal antibody (2AC2). Control muscles were incubated with 100 μg/ml unlabeled antibody for 1 h and then in medium containing both 5 μg/ml iodinated antibody and 100 μg/ml unlabeled antibody. Incubation was for 4 h at 20°C. Muscles were then rinsed extensively to remove unbound antibody, including an overnight rinse in ~1 liter of medium at 4°C. Total binding per muscle was estimated by gamma scintillation spectrometry and nonspecific binding found to be ~15% of specific binding.

The muscles were then fixed in 2% glutaraldehyde, 0.1 M cacodylate buffer, pH 7.5, postfixed in 1% osmium tetroxide, and dehydrated and embedded in Epon. Pale gold sections were cut for electron microscope autoradiography and 1-μm sections for light microscope autoradiography. For light microscope autoradiography, sections were mounted on glass slides and coated in Kodak NTB-2 emulsion. Autoradiographs were developed in D-19 developer for 2.5 min at 20°C. For electron microscope autoradiography sections were mounted on Formvar-coated grids, stained with lead citrate, and shadowed with carbon. The grids were coated with Ilford L-4 emulsion by the loop method (33) and autoradiographs were developed in D-19 developer.

Quantitative Analysis of Electron Microscope Autoradiographs: Two types of quantification were performed. First, the method of Salpeter et al. (34) was used to analyze the distribution of silver grains with respect to the plasma membrane in extrajunctional areas of muscle fibers. Electron micrographs were prepared at an initial magnification of 5,600 and were printed at a final magnification of 18,300. Each silver grain was circumscribed by the smallest possible circle. A transparent plastic sheet inscribed with concentric circles was then placed over each circle and its center marked on the micrograph with an insect pin. Under a dissecting microscope with eyepiece-equipped micrometer, the distances were measured from the center of each encircled grain to the plasma membrane.

The second type of analysis consisted of a comparison between the density of silver grains in the basal lamina along endplate and non-endplate surfaces of muscle fibers. For this procedure only fibers that had neuromuscular junctions in the plane of section were used. We recorded each such fiber in a series of overlapping micrographs at × 4,200. The negatives were assembled into a montage and the surface of each fiber was traced onto clear plastic film. All silver grains within several grain diameters of the basal lamina were marked on the tracing. Each negative was also enlarged to a final magnification of 91,000 by projection onto a ground glass plate, and the center of each silver grain determined as the center of the smallest circumscribing circle. The distance from each grain center to the plasma membrane was then measured. All silver grains whose centers fell within 165 nm of the center of the basal lamina were scored and marked on the whole fiber tracings. The length of nonsynaptic basal lamina was measured with a planimeter, and used to calculate the density of grains per unit length of basal lamina.

To measure grain densities within synaptic regions required a more complex procedure because of the complicated folding of the muscle cell surface. Each silver grain at sites of nerve-muscle contact was included in the count if its center, determined as described above, was within 165 nm of the center of any portion of the muscle basal lamina adjacent to a nerve terminal or its Schwann cell sheath. For this analysis, each synaptic region was projected onto paper and traced at a final magnification of 42,000 so that the total length of basal lamina in all of the junctional folds could be measured by planimetry. The increase in basal lamina area attributable to infoldings of the plasma membrane in synaptic regions was estimated by comparing the total length of basal lamina in synaptic sites to the length of a line constructed across the tops of the corresponding postsynaptic folds, connecting the extrajunctional basal lamina at each side of the neuromuscular junction.

It was clear from light microscope autoradiography of the control muscle that had been exposed to unlabeled antibody before incubation with ^{125}I-conjugated antibody (data not shown) that the vast majority of nonspecific binding was associated with the muscle fascia. A low level of nonspecific binding also occurred in other collagen-rich areas of extracellular matrix visible in electron microscope autoradiographs. However these collagen fibrils existed at much greater distances from the basal lamina than the silver grains due to specific antibody binding, and appeared virtually unlabeled at the exposure times used for quantitation.

RESULTS

Hybridoma techniques have been used to generate a variety of cell lines secreting monoclonal antibody specific for *X. laevis* antigens. Through the use of contrasting fluorochromes during the initial screening procedure, it was possible to select from these a library of four hybridoma lines generating antibodies to antigen(s) that appeared to be concentrated at the neuromuscular junction (see below). These antigens were presumed to be associated with basal lamina because their extrasynaptic tissue localization appeared similar to the pattern of immunocytochemical staining reported for laminin (35) and type IV collagen (36). For control experiments, two additional hybridoma lines were selected that secreted antibodies against antigens that appeared abundant in the extracellular matrix between muscle fibers. Labeling with these antibodies was not conspicuous in regions stained by TRITC-labeled αBGT that binds selectively to AChR, concentrated in the postsynaptic membrane (23). Further screening on cryotome sectioned adult muscle indicated that these latter antibodies showed no detectable binding to chicken muscle. However, all could bind to muscles of *Rana catesbiana*, although two of them did so at notably reduced levels (data not shown). The strategy of subsequent experiments was to use the purified monoclonal antibodies both to identify the relevant antigens and to determine antigen organization in muscle tissue.

Immunochemical Identification of Basal Lamina Antigens

In our attempt to identify the molecular species recognized by each antibody, a problem was posed by the suspected association of the antigens with the highly insoluble extracellular matrix. Isolation of individual proteins from extracellular matrix requires the use of chaotrophic agents that disrupt the adhesive molecular interactions maintaining matrix organization. Such extraction conditions run the risk of altering or destroying the tertiary molecular structure often important for antigen-antibody recognition. This can introduce hazards for the use of monoclonal antibodies, because they are directed against only a single immunological determinant, which may be conformation-dependent. To circumvent this problem, we exploited the fact that many connective tissue components are also secreted as soluble products by cells developing in culture. Notable examples include several collagen types (37, 38) AChE (39), fibronectin (40), laminin (41, 42), sulfated glycoproteins (43, 44), and a variety of proteo-

glycans (45, 46). Because the secretory products of cells developing in culture can be labeled metabolically with radioactive precursors, it was possible to generate a highly diluted solution of labeled extracellular matrix components without recourse to chemical denaturants. Conventional immunochemical techniques that involve precipitation of monoclonal murine immunoglobulin with goat anti-mouse IgG antiserum (see Materials and Methods) could then be used to isolate the labeled antigens for biochemical analysis.

For this purpose immune precipitation was carried out in conditioned medium that had been prepared by growing dissociated *Xenopus* embryonic tail cells in the presence of [^{35}S]methionine. Fig. 1 shows fluorographs of SDS polyacrylamide gels containing the labeled proteins precipitated by each of the presumptive anti-basal lamina antibodies, as well as another (control) antimatrix immunoglobulin (designated 1AC5) and a negative control provided by monoclonal IgG from the MOPC-21 myeloma. In this experiment the proteins were analyzed under reducing conditions. The MOPC-21 immunoglobulin (Fig. 1 *h*) and other irrelevant monoclonal antibodies (not shown) precipitated no detectable labeled bands. However, the antibodies directed against extracellular matrix antigens from *X. laevis* did precipitate labeled material. In fact, each of the antibodies that showed an apparent basal lamina localization upon immunofluorescent screening also precipitated an identical complex of broad bands, which were of high molecular weight but able to enter the resolving gel (Fig. 1, *b–e*). No labeled material was detectable in the stacking gel (data not shown). Each of these bands appeared substantially larger than the proteins commonly employed as molecular weight markers (M_r ≤230,000) and also showed a conspicuous heterodispersity suggestive of extensive glycosylation. This was in marked contrast to the pattern of labeled components precipitated by the control antimatrix antibody (1AC5), which consisted of a relatively narrow high molecular weight band, and an array of smaller and less intensely labeled subordinate bands (Fig. 1, *a* and *g*). In all cases, the relative prominence of the lower molecular weight bands also varied between experiments (see Fig. 1, *b* and *f* and *a* and *g*). These characteristics suggested that each antibody was precipitating a single high molecular weight antigen, together with an assortment of its proteolytic breakdown products. This was confirmed by analysis of the precipitated antigens under nonreducing conditions (see below). During these experiments no qualitative difference was noted between the material precipitated by the four presumptive basal lamina antibodies. While the electrophoretic patterns were essentially identical, the quantity of material precipitated by each antibody did vary (Fig. 1, *b–e*). One antibody (designated 2AC2) was thus selected for subsequent, more detailed analysis (see below).

The large size and conspicuous polydispersity of the [^{35}S]-methionine labeled bands precipitated with the monoclonal anti-basal lamina antibodies suggested that the antigenic species might be a proteoglycan. This family of heavily glycosylated proteins is known to be present in extracellular matrices and can be distinguished experimentally from most other glycoproteins by an abundance of anionic sulfate associated with the glycosaminoglycan side chains (for reviews, see references 45, 47). This characteristic allows proteoglycans to be preferentially labeled by the growth of cultured cells in medium supplemented with [^{35}S]sulfate. Fluorographs of *Xenopus* conditioned medium which had been labeled either with [^{35}S]methionine, or [^{35}S]sulfate, and analyzed without reduction on SDS-containing 3–15% polyacrylamide gradient gels are presented in Figs. 2, *c* and *f*, and 3, *c* and *f*. As expected, the dominant components labeled by [^{35}S]sulfate were different from those labeled by [^{35}S]methionine, both in size and dispersity during gel electrophoresis. By far the greatest sulfate labeling was found in material trapped at the origin in the 3% acrylamide stacking gel (Fig. 3, *c* and *f*). This would be expected to consist primarily of large chondroitin (dermatan) sulfate proteoglycans (M_r ≥1,000,000) known to be secreted by connective tissue cells in culture (45). In addition to this major component, a number of smaller species were detected in the resolving gel. Most of these show the broad, heterodis-

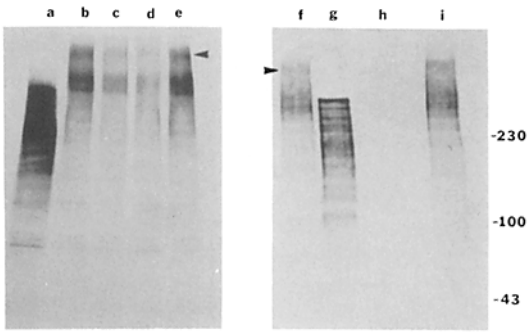

FIGURE 1 Fluorographs of [^{35}S]methionine-labeled products precipitated from *Xenopus* cell conditioned medium by different monoclonal mouse antibodies, analyzed on 3–15% polyacrylamide gradient SDS gels after reduction. Lanes *a–e* and *f–i* represent separate experiments analyzing the entire immune precipitate obtained from 0.5 ml conditioned medium. Lanes *b*, *f*, and *i* show material precipitated by antibasal lamina antibody 2AC2; lanes *c*, *d*, and *e* material obtained with similar antibodies 2AA5, 2BD5, and 2BA5, respectively; lanes *a* and *g* show precipitate of the control *Xenopus* extracellular matrix antibody 1AC5; lane *h*, corresponding precipitate of the monoclonal antibody of the MOPC-21 myeloma. Arrows indicate the position of the same major band in each fluorograph.

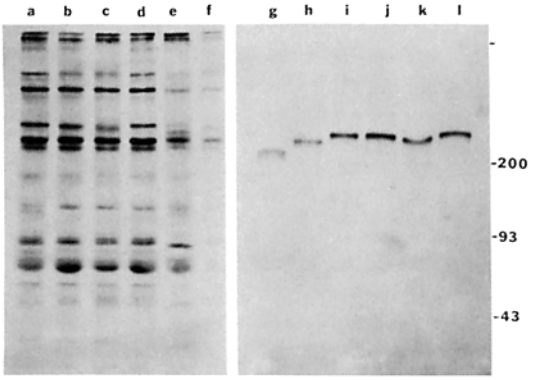

FIGURE 2 Fluorographs of [^{35}S]methionine-labeled *Xenopus* secreted proteins after exposure to different glycosaminoglycan lyases and analysis on 3–15% SDS PAGE without reduction. Lanes *a–f* show the major constituents of unfractionated [^{35}S]methionine-conditioned medium, and lanes *g–l* the labeled antigen precipitated by extracellular matrix antibody 1AC5. Lanes *c*, *f*, and *l* show controls incubated without enzyme (lane *f* contained 25% the volume of *c*); lanes *a*, *b*, *i*, and *k* similar amounts of starting material as in *c* and *l*, after treatment with heparinase (see Materials and Methods); lanes *d* and *j*, after chondroitinase ABC; lanes *e* and *h*, after keratinase; lane *g*, after hyaluronidase. Note the absence of effect of heparinase and chondroitinase ABC on electrophoretic mobility, compared with keratanase or hyaluronidase. Also note the conspicuous difference in dispersity of 1AC5 antigen when analyzed without reduction (compared with Figure 1, *a* and *g*).

perse band structure characteristic of proteoglycans.

Immune precipitates from [^{35}S]sulfate labeled conditioned medium are shown in Fig. 4, *b*, *g*, and *h*, analyzed with and without reduction. In this experiment, neither the MOPC21 nor the control matrix antibody (IAC5) precipitated detectable labeled material (data not shown). In contrast, 2AC2 (Fig. 4, *b*, *g*, and *h*) and each of the other presumptive anti-basal lamina antibodies (data not shown) precipitated similar heterodisperse bands whose major component showed the same electrophoretic mobility as that obtained from [^{35}S]methionine-labeled medium (Fig. 1). Labeled material was not detected in the stacking gel (not shown). These observations strongly suggest that each of these antibodies recognizes a similar high molecular weight proteoglycan (M_r ≃430,000–580,000) secreted by cultured *X. laevis* cells.[2]

Effect of Reduction on Antigen Electrophoretic Mobility

Electrophoretic analysis of each of these metabolically labeled antigens under conventional, reducing conditions produced a complex of labeled bands. The relative intensity of these bands varied between experiments (compare Fig. 1, *b*, *f*, and *i*) in a manner that suggested that the band-heterogeneity resulted from proteolytic degradation of the antigen, rather than from the presence of disulfide-linked antigen subunits. This became obvious when the antigens were analyzed under identical electrophoretic conditions, but without reduction in mercaptoethanol. Comparison of the control lanes in Figs. 4*h* and 5, *a* and *g*, with the reduced antigen shown in Figs. 1, *b*, *f*, and *i* and 4*b* and *g*, shows the pronounced effect reduction has upon the electrophoretic mobility of the basal lamina proteoglycan and the control matrix antigen 1AC5 (compare Figs. 1, *a* and *g*, and 2*l*). When either of the labeled antigens was precipitated from [^{35}S]methionine-labeled culture medium and analyzed under nonreducing conditions, virtually all of the lower molecular weight species (see Fig. 1) disappeared. Furthermore, the original band of highest molecular weight increased slightly in electrophoretic mobility and became intensely labeled (requiring ~20% the original exposure time). These observations indicate that the secreted form of each of these high molecular weight antigens had undergone limited attack by endopeptidases, probably during the extended period of metabolic labeling, but appeared intact in Figs. 2–5 because of residual intramolecular disulfide bonding between the peptide fragments.

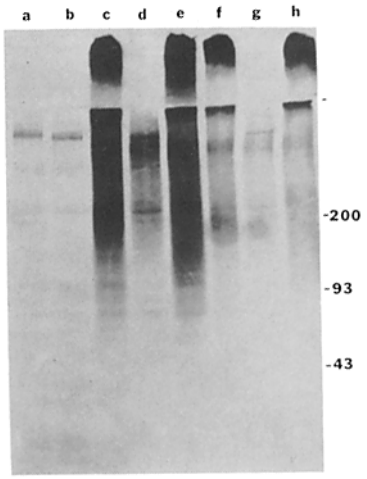

FIGURE 3 Fluorograph of [^{35}S]sulfate-labeled *Xenopus* secreted products after exposure to different glycosaminoglycan lyases and analysis on 3–5% SDS PAGE without reduction. (The 3% acrylamide stacking gel is retained to show very high molecular weight proteoglycans trapped at the origin.) Lanes *a–e* represent fourfold the amount of starting material as lanes *f–h*. Lanes c and *f* show controls incubated without enzyme; lanes *a* and *b* after heparinase; lanes *d* and *g* after chondroitinase; and lanes e and *h* after keratanase. Note removal of label from the stacking gel by chondroitinase ABC, and heparinase (known to be contaminated with chondroitinases) but not by keratanase. Note also removal of label by heparinase from several of the bands in the resolving gel that were spared by chondroitinase ABC.

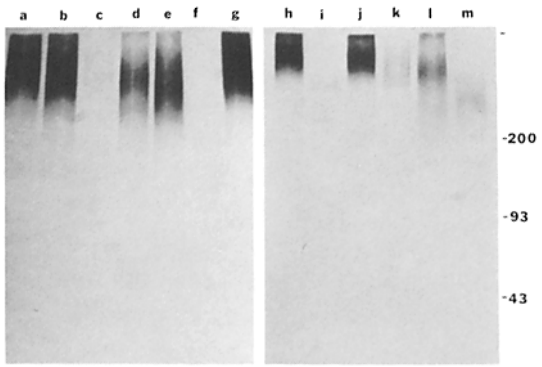

FIGURE 4 Fluorographs of [^{35}S]sulfate-labeled *Xenopus* basal lamina antigen precipitated by monoclonal antibody 2AC2, and treated with different glycosaminoglycan lyases. Lanes *a–g* and *h–m* show similar analyses on 3–15% SDS PAGE respectively with and without reduction. Lanes *b*, *g*, and *h* show controls incubated without enzyme; lanes *c*, *f*, *i*, *k*, after heparinase; lanes *a* and *j*, after chondroitinase ABC; lanes e, *l*, after keratanase; and lanes *d* and *m*, after hyaluronidase. Note the almost complete removal of [^{35}S]-sulfate by heparinase, but not by chondroitinase or keratanase. Note also the increase in antigen dispersity brought about by reduction.

Enzymatic Degradation of Labeled Antigen

We carried out further analysis on the structure of the basal lamina proteoglycan employing enzymes that selectively de-

[2] Such electrophoretic estimates of apparent molecular weight for the basal lamina proteoglycan recognized by antibody 2AC2 are, of necessity, relatively crude. Without appropriate markers in the 500,000 mol-wt range, it is unclear, for example, whether this region of the gel shows major departures from the linearity observed with conventional lower weight protein standards. Furthermore, even if appropriate markers of very high molecular weight were available, the existence of extended polyanionic saccharide side-chains would be expected to alter the electrophoretic properties of proteoglycans relative to conventional proteins. Additional complexity is introduced by the fact that the best electrophoretic resolution was obtained under nonreducing conditions, which would be expected to decrease the hydrated radius of the isolated antigens relative to the random coil structures of reduced protein standards. By ignoring such uncertainties, one can generate apparent molecular weight values suitable as approximations and for comparisons between different laboratories. Such values range from a high of 580,000 mol wt for the trailing edge of the largest fragment of the reduced proteoglycan precipitated by antibody 2AC2, to a low of 430,000 mol wt for the leading edge of the same species analyzed without reduction. Similar high and low values for the heparinase resistant domain (see below) of the proteoglycan are 440,000 and 340,000 mol wt, respectively. For the control matrix antigen 1AC5, corresponding values are 370,000 and 260,000 mol wt.

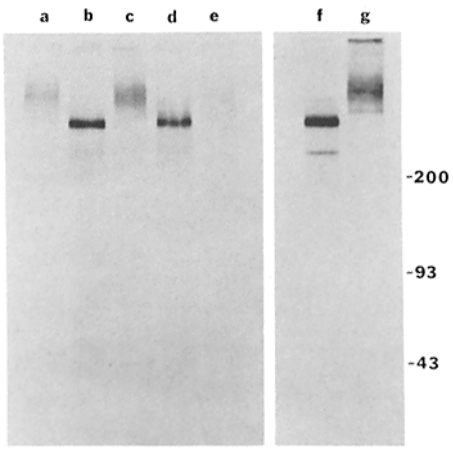

FIGURE 5 Fluorographs of [^{35}S]methionine-labeled *Xenopus* basal lamina antigen precipitated by monoclonal antibody 2AC2 and treated with different glycosaminoglycan lyases. Immune precipitates were analyzed on 3–15% SDS PAGE without reduction. Lanes *a* and *g* show controls incubated without enzyme; lanes *b* and *d*, precipitates treated with heparinase; lane *c*, treated with chondroitinase ABC; lane *e*, treated with keratanase; lane *f*, immune precipitate obtained from conditioned medium previously treated with heparinase (see Fig. 2, *a* and *b*). Note both the increase in electrophoretic mobility and decrease in polydispersity brought about by heparinase, but not chondroitinase ABC. Note also the increase in electrophoretic dispersity caused by reduction (compare Fig. 5, *a* and *g*, with Fig. 1, *b*, *f*, and *i*).

grade the glycosaminoglycan side chains which characterize different classes of proteoglycan. Earlier studies have analyzed the chemical composition of the proteoglycans that are present in basal laminae. These studies have either examined the effects of glycosidases on cytochemical staining of polyanions, characterized the residue of glycosaminoglycan that remains after extraction and proteolytic degradation, or, more recently, attempted to isolate intact proteoglycans (49–55). Such analysis has revealed that basal laminae contain proteoglycans of two principal classes, characterized by side chains of chondroitin (dermatan) sulfate or heparan sulfate. These glycosaminoglycans also exist in amphibian muscle (56) and can be distinguished experimentally by various chemical tests, including their differential susceptibility to chondroitinase ABC (28). It is also possible to supplement this analysis by degradation of some heparan sulfates with bacterial heparinase or heparitinase (30). To characterize the antigen recognized by our monoclonal antibodies, immune precipitates of the metabolically labeled *Xenopus* basal lamina proteoglycan were analyzed by SDS gel electrophoresis after treatment with these enzymes.[3] As controls, degradation was also attempted with *Streptomyces* hyaluronidase and *Pseudomonas* keratanase (57).

[3] This form of analysis is based upon the expectation that the appropriate lyase will degrade the precipitated proteoglycan to a domain composed primarily of its protein core. Upon electrophoretic analysis in SDS, the deglycosylated proteoglycan would be expected to increase in mobility and assume a less disperse band-structure. Furthermore, the progress of such a deglycosylation reaction can be directly monitored since proteoglycans can be labeled either in their core proteins, via [^{35}S]methionine, or in their glycosaminoglycan side-chains, via [^{35}S]sulfate. Deglycosylation can thus be visualized as a loss of [^{35}S]sulfate from the labeled proteoglycan band, without a corresponding loss of [^{35}S]methionine.

The activity of each lyase was also tested on the entire complement of metabolically labeled *Xenopus* secretory products. These experiments served to ensure that the commercial enzyme preparations were active, and reveal the extent to which they were contaminated with proteases or glycosidases of inappropriate specificity. The effects of these enzymes on the secreted products of *Xenopus* cultures are presented in Figs. 2 and 3. Protease contamination was also tested by exposure of immune precipitates of [^{35}S]methionine labeled control matrix antigen (IAC5) to each enzyme (Fig. 2, *g–l*). Since none of the conspicuous species in either of these methionine-labeled preparations appear to be proteoglycans, no change in their labeling intensity or electrophoretic mobility would be expected if the enzymes contained only the specified glycosidase activity. These tests did, in fact, reveal substantial protease contamination of the enzyme hyaluronidase (Fig. 2, *f* and *g*), and lesser protease contamination of keratanase (Fig. 2, *e* and *h*). In contrast, chondroitinase ABC (Fig. 2, *d* and *j*) and two separate preparations of heparinase (Fig. 2, *a*, *b*, *i*, and *k*) showed no detectable protease activity. When the same enzymes were applied to [^{35}S]sulfate-labeled culture medium, their effects appeared quite different (Fig. 3). As predicted from their observed protease contamination, the control enzymes, keratanase (Fig. 3, *e* and *h*) and hyaluronidase (not shown), both increased the electrophoretic mobility and reduced the intensity of ^{35}S-labeling in several bands. Chondroitinase ABC abolished sulfate-labeling from the major, very high molecular weight species trapped at the top of the stacking and resolving gels (Fig. 3, *d* and *g*), but spared a group of smaller proteoglycans within the resolving gel. Both of the heparinase preparations (which may be contaminated with heparitinase and chondroitinases) abolished [^{35}S]sulfate labeling (Fig. 3, *a* and *b*) in both the very large and several of the smaller proteoglycans.[4] Heparinase thus showed specificity in removing [^{35}S]sulfate labeling from the major [^{35}S]sulfate-labeled bands, while sparing other discrete minor components. The action of the heparinase preparations used in this study (see below) is thus unlikely to be the result of any contamination with proteases or nonspecific sulfatases. Those sulfate-labeled bands removed by heparinase, but not by chondroitinase ABC or keratanase, are likely to represent heparan sulfate proteoglycans.

Similar enzyme treatments were used to degrade the metabolically labeled *Xenopus* antigen precipitated by the anti-basal lamina proteoglycan antibody (2AC2). Results of such an experiment are presented in Figs. 4 and 5, analyzed under nonreducing conditions. Specific glycosidase effects are best revealed by comparison of the changes in labeling intensity and electrophoretic mobility of the basal lamina proteoglycan in parallel methionine (Fig. 5) and sulfate (Fig. 4) gels. As expected from its protease contamination (see above) the control enzyme, hyaluronidase, greatly reduced the intensity of both sulfate and methionine label (data not shown). Likewise, keratanase produced corresponding reductions in the intensity of both labels but caused little change in electrophoretic mobility or dispersity of the labeled proteoglycan (Figs. 4, *e* and *l*, and 5 *e*). In contrast, chondroitinase ABC had no detectable effect on the mobility or intensity of the basal lamina proteoglycan labeled with either sulfate or methionine (Figs. 4, *a* and *j*, and 5 *c*). These observations indicate that

[4] A new band also appeared in heparinase and chondroitinase-treated lanes, possibly reflecting residual chondroitin sulfate associated with the major proteoglycan originally trapped at the gel origin.

this basal lamina antigen is unlikely to be either a keratan sulfate, dermatan sulfate, or chondroitin sulfate proteoglycan, and thus suggest that it is a heparan sulfate proteoglycan. This was confirmed by the observation that both preparations of heparinase greatly reduced the extent of antigen labeling with sulfate but not methionine (Figs. 4, *c*, *f*, *i*, and *k*, and 5, *b* and *d*). Instead, the methionine-labeled antigen was reduced in apparent molecular weight, and showed a notable loss of heterodispersity. This produced a much narrower band which actually appeared more intensely labeled. This is illustrated quantitatively in Fig. 6 which compares densitometric scans through two lanes of the fluorograph in Fig. 5. Heparinase thus produced changes in both the electrophoretic mobility and peak-shape of the methionine-labeled antigen, increasing height at the expense of width, while removing virtually all sulfate. These are exactly the effects that would be predicted from deglycosylation of a heparan sulfate proteoglycan, leaving a residue composed primarily of core-protein.[5]

While its differential sensitivity to degradation with chondroitinase, keratanase, and heparinase indicates that the basal lamina antigen recognized by these monoclonal antibodies is probably associated with a large heparan sulfate proteoglycan, such experiments do not indicate whether the antigenic site on the molecule recognized by this monoclonal antibody (2AC2) is associated with the core protein or its glycosaminoglycan side chains. To distinguish between these alternatives, [^{35}S]methionine-labeled conditioned medium was treated with heparinase (see Fig. 2, *a* and *b*) and then subjected to immune precipitation with monoclonal antibody (2AC2). As shown in Fig. 5*f*, prior treatment with heparinase did not prevent antigen precipitation, but the precipitated species showed electrophoretic properties similar to those obtained when the antigen was treated with the enzyme after immune precipitation. This result would only be expected if the antigenic site for this monoclonal antibody resided on a heparinase-insensitive domain of the proteoglycan, associated with either the core protein or oligosaccharide side chains.

Fluorescence Immunocytochemical Staining of Adult Frog Muscle

Initial screening of the hybridoma conditioned medium by indirect immunofluorescence indicated that four separate cell lines were secreting antibody that appeared to stain basal laminae, and showed enhanced binding to *Xenopus* larval neuromuscular junctions, revealed by counterstaining with TRITC-labeled αBGT. However, in the (10-μm) transverse sections of larval tail muscle, each presumptive anti-basal lamina antibody also showed extensive binding to the entire muscle surface, nerve fibers, blood vessels, and the outer surface of the notochord (data not shown). To determine the organization of the proteoglycan on the muscle fiber surface more precisely, we stained intact adult *Xenopus* sartorius muscles with FITC-labeled monoclonal antibody (2AC2) followed by FITC-labeled goat anti-mouse IgG. The dense array of postsynaptic AChR was again identified by counterstaining the muscle with TRITC-labeled αBGT. After brief fixation in 2% wt/vol formaldehyde, individual muscle fibers and small fiber bundles were dissected and examined in the fluorescence microscope (Fig. 7). This procedure allowed the surface of individual stained muscle fibers to be viewed face-on, revealing local variations in apparent antigen site-density. When viewed in this manner, the antigen was found to be organized in a diffuse fibrous felt-work over the enzire muscle surface (not visible in Fig. 1). At the neuromuscular junction, however, the antibody-staining showed an abrupt increase in intensity adjacent to the post-synaptic membrane visualized by TRITC-αBGT (Fig. 7, *b* and *d*). This increase in staining intensity was evident within and between the secondary junctional folds (seen as irregular vertical banding in Fig. 7, *c* and *d*). The organization of antigen and the postsynaptic clusters of AChR showed extensive homology, but their distributions were not identical. While all regions of junctional AChR staining were associated with adjacent dense accumulations of antigen, sites of apparently high antigen-density within the neuromuscular junction (Fig. 7*c*) frequently occurred without corresponding AChR stain (Fig. 7*d*). This phenomenon was most conspicuous at the tips of individual terminal branches where antigen-plaques sometimes extended well beyond the region stained by TRITC-αBGT. In this regard the antigen distribution was reminiscent of AChE-stained frog muscle fibers. This histochemical procedure produces reaction product which sometimes extends beyond the tips of nerve-terminals (59). In occasional instances entire terminal branches of a neuromuscular junction appeared intensely stained with antibody but devoid of AChR clusters (data not shown). These characteristics of antigen organization will be described more completely in a future report (D. C. Linden and M. J. Anderson, in preparation).

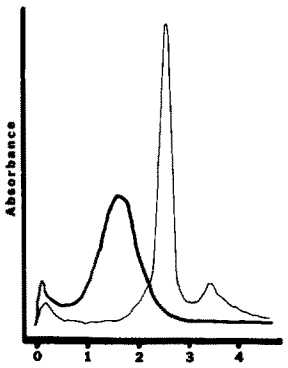

FIGURE 6 Densitometric scans of fluorographs of [^{35}S]methionine-labeled antigen precipitated by monoclonal antibody 2AC2, before (heavy line) and after degradation with heparinase. Absorbance of the fluorograph is plotted as a function of electrophoretic mobility (in centimeters on a 13-cm gel) on SDS PAGE, 3–15% gradient gel.

Electron Microscope Autoradiography

While the staining shown in Fig. 7 strongly suggests that the proteoglycan antigen identified (see above) by this monoclonal antibody (2AC2) is heavily concentrated at the neuromuscular junction, this form of cytochemical experiment is subject to artifacts introduced by the complex surface geometry of the synaptic region. Invagination of the muscle surface, introduced both by the synaptic gutter and the 1–2 μm deep junctional folds, would be expected to accentuate the apparent antigen site-density seen from the almost two-dimensional

[5] Chondroitinase ABC has been shown to degrade chondroitin 4-sulfate, chondroitin 6-sulfate and dermatan sulfate (28). Crude extracts of *F. heparinum* are contaminated with chondroitinases, and heparitinase, but are free of protease, collagenase, sialidase, and fucosidase activities (29–31). While specific for glycosaminoglycans, such potential contaminants of heparinase can degrade all glycosaminoglycan species except keratan sulfate. In our study, therefore, we compared the action of heparinase to parallel treatments with chondroitinase ABC and keratanase. Since the effect of heparinase on the electrophoretic behavior of the basal lamina antigen could not be duplicated by either of these enzymes, it is likely to have resulted from either heparinase itself, or some residual contaminant heparitinase.

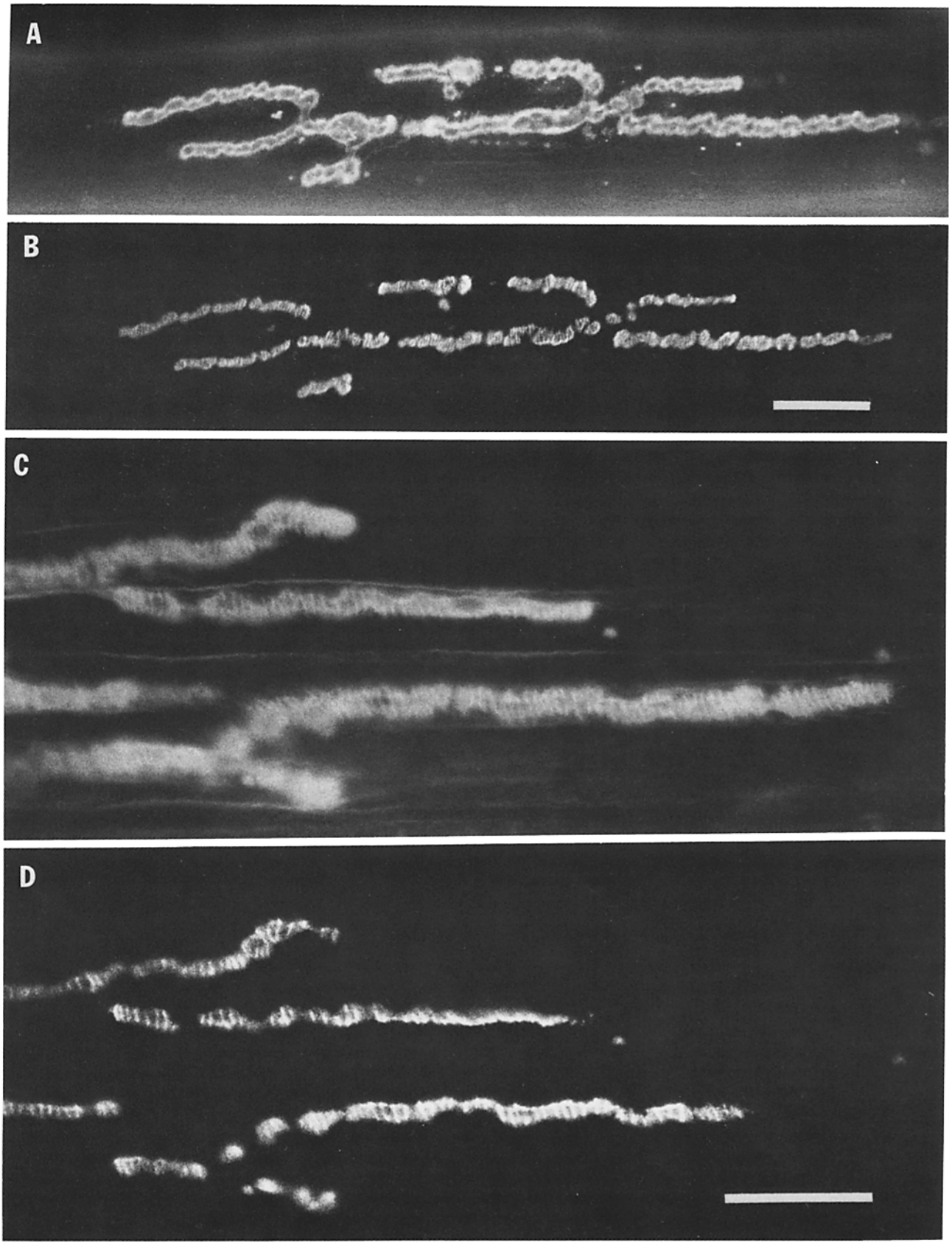

FIGURE 7 *Xenopus* sartorius muscle fibers stained with monoclonal antibody (2AC2) followed by FITC-labeled goat anti-mouse IgG (*A* and *C*), and counterstained with TRITC-labeled α-bungarotoxin (*B* and *D*) to reveal the postsynaptic accumulation of ACh receptors. The dense accumulation of antigenic sites is conspicuous throughout the postsynaptic region, including the periodic bands due to invagination of the muscle surface. Note also that the postsynaptic region labeled by the antibody (*A* and *C*) commonly extends beyond the dense ACh receptor array both laterally and at the tips of individual terminal branches (*C* and *D*). Bars, 30 μm. (*A* and *B*) × 570. (*C* and *D*) × 880.

perspective of the light microscope. Ultrastructural immunocytochemistry was thus carried out both to determine the site of antigen localization on the muscle cell surface, more precisely, and to estimate the extent of its concentration in the vicinity of the neuromuscular junction. Electron microscope autoradiography, after exposure to ^{125}I-labeled antibody, is particularly useful since it provides quantitative data concerning local variations in antigen site-density, while minimizing artifacts attributable to steric hinderance of antibody-derivative penetration into a complex structure. We thus exposed adult *Xenopus* sartorius muscle to ^{125}I-labeled antibody (2AC2) and used the method of Salpeter et al. (34) to analyze electron microscope autoradiographs and plot the variation of silver grain density at different distances from the plasma membrane (see Materials and Methods). We performed this analysis on 466 silver grains in 64 micrographs prepared at a final magnification of 18,300. Figs. 8 and 10 illustrate typical examples of such autoradiographs, and Fig. 9 shows the distribution of grain centers about the plasma membrane. The approximate thickness and position of the basal lamina are indicated by hatch marks. The grain distribution shows a single peak displaced from the plasma membrane and centered over the basal lamina. More distant structures of the extracellular matrix appeared virtually unlabeled at the exposure times used for the preparation of these micrographs. Taken together, these findings are most consistent with a principle antigen localization within the muscle basal lamina, rather than either the plasma membrane or more distal extracellular matrix. Similar autoradiographic analyses have previously been used to localize AChR and AChE in the muscle plasma membrane and basal lamina respectively (1, 4). As expected, accumulations of silver grains could also be seen in association with the basal laminae of small blood vessels running between some muscle fibers (data not shown). Silver grains were likewise found associated with the extrasynaptic Schwann cell basal lamina at the neuromuscular junction.

We used a different type of quantitative analysis to compare the concentrations of antigen in synaptic and adjacent extrajunctional regions of muscle fiber basal lamina (see Materials and Methods). For this analysis we used only muscle fibers sectioned through the endplate region. This involved a total of 21 fiber profiles with 38 distinct regions of synaptic contact (Fig. 10). To avoid complications introduced by the boundary zone between junctional and extrajunctional basal lamina (see Fig. 7), we excluded the extrajunctional cell surface within 3 μm of each synaptic contact from analysis. Such calculations indicate that the synaptic basal lamina shows an approximately 16-fold higher apparent concentration of antigen sites relative to the extrajunctional muscle surface. However, since

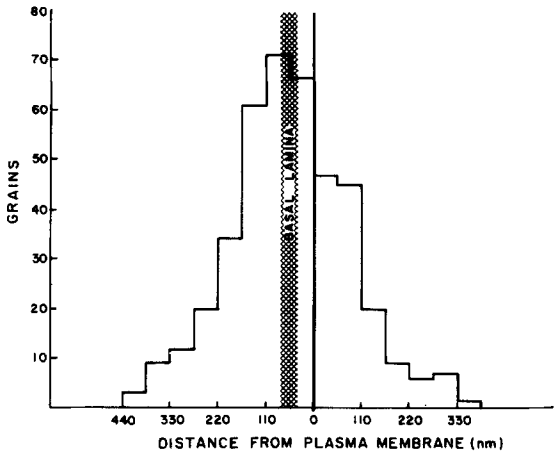

FIGURE 9 Frequency histogram of autoradiographic grain-centers about the muscle fiber plasma membrane. Note the displacement of grain-distribution away from the plasma membrane toward the adjacent basal lamina (hatch marks).

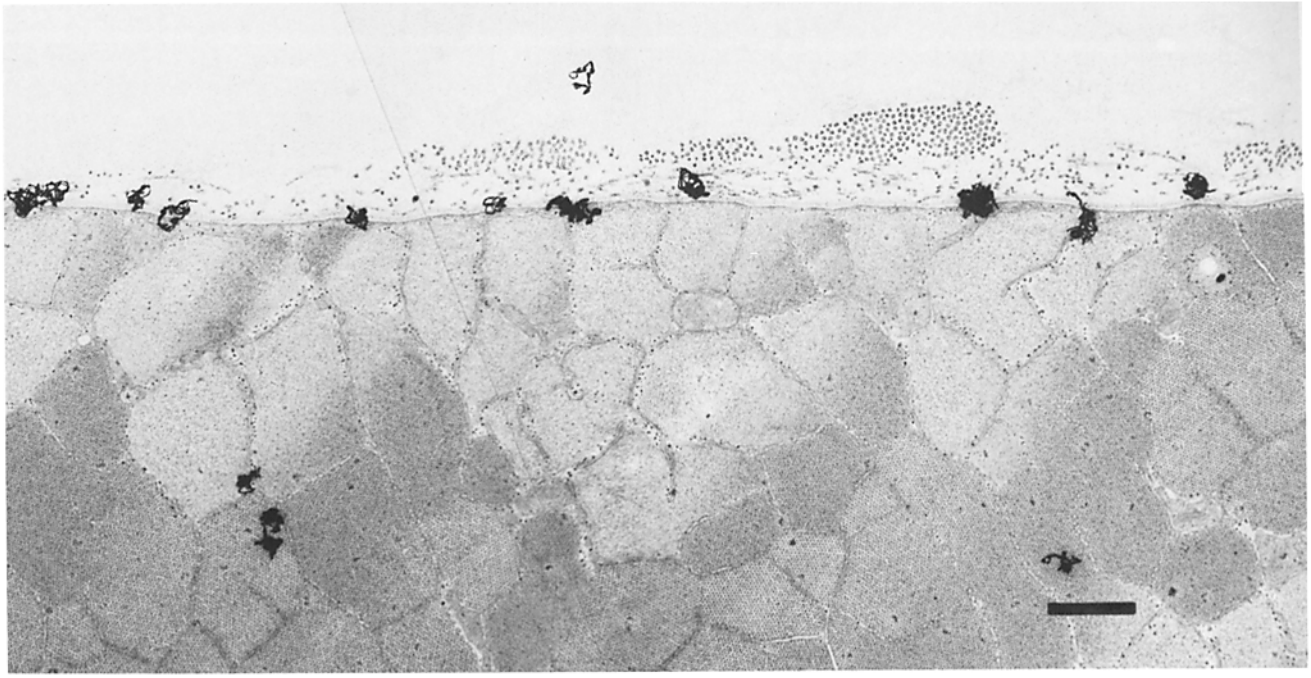

FIGURE 8 Electron microscope autoradiograph of *Xenopus* sartorius muscle fiber sectioned transversely after labeling with ^{125}I-conjugated monoclonal antibody (2AC2). Note the association of most silver grains with the muscle fiber surface rather than the cytoplasm or more distal elements of extracellular matrix. Bar, 1.0 μm. × 11,500.

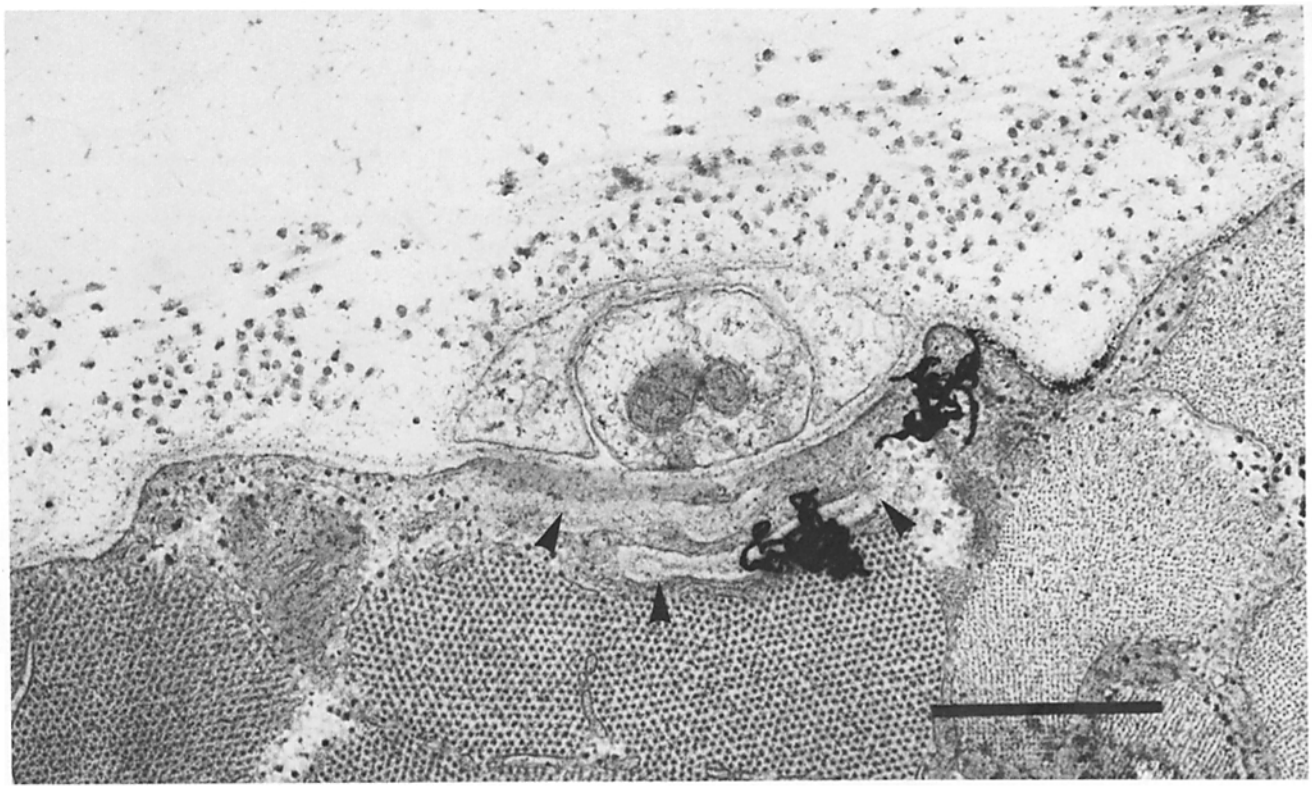

FIGURE 10 Electron microscope autoradiograph of ^{125}I-labeled antibody binding at the *Xenopus* sartorius neuromuscular junction. The micrograph shows a single nerve terminal surrounded by a Schwann cell sheath and a complex array of extracellular matrix fibrils. In such autoradiographic exposures silver grains were found to be concentrated fivefold within the postsynaptic region, including the deep secondary invaginations of muscle surface (arrows). Bar, 1.0 μm. × 31,000.

the muscle fiber surface area also appears to be increased threefold by infoldings of the plasma membrane at the neuromuscular junction, the net increase in antigen site-density at the synapse has been estimated to be approximately 5.3-fold. This calculation assumes that all junctional antigenic sites are as available to the labeled antibody as sites on the remainder of the cell surface. It remains possible, however, that extrajunctional antigenic sites are more accessible than junctional sites, particularly those located within the depths of secondary folds. Conceivably, the binding of antibody in the primary synaptic cleft might even sterically hinder antibody access to deeper regions of synaptic infolding. Junctional antigenic sites of intact muscle may therefore be difficult or even impossible to saturate with monoclonal antibody. For these reasons our calculation of a 5.3-fold increase in antigen density at the neuromuscular junction may well be an underestimate of the actual antigen concentration in this region.

Proteoglycan Organization on Embryonic Muscle in Cell Culture

Cytochemical examination of basal lamina proteoglycan organization in adult frog muscle has revealed a diffuse distribution over the entire muscle fiber surface, and dense plaques associated with the chemically specialized basal lamina at the neuromuscular junction (Figs. 7–10) and the myotendonous junction (data not shown). This localized concentration of antigenic sites at the neuromuscular junction suggested that the organization of basal lamina proteoglycan might be regulated by nerve-muscle interaction during embryonic development. This possibility was evaluated by examining the distribution of the proteoglycan on embryonic *X. laevis* myotomal muscle cells developing in culture with or without nerve cells. Previous studies of this preparation have indicated that developing cholinergic neurons establish functional neuromuscular junctions (13, 59, 60) with morphological characteristics similar to those found in the developing embryo (61). These studies have also indicated that functional neuromuscular junctions can be identified on cultured muscle cells by the presence of morphologically characteristic AChR clusters along paths of nerve-muscle contact (13, 60).

When muscle cultures, grown without neural tissue, were stained with FITC-labeled monoclonal antibody (in some cases amplified by further exposure to FITC-labeled goat anti-mouse immunoglobulin), we found the embryonic muscle cells had a pattern of surface staining quite different from that seen on adult muscle fibers (Fig. 7). The background of diffuse labeling was notably less conspicuous than that observed in adult muscle, and the stain consisted primarily of a complex array of dense antigen plaques and fibrils (Fig. 11*a*). The number and organization of plaques varied greatly between cells, but there was a tendency for them to occur preferentially on the cell surface facing the collagen substrate, particularly near the tips of cell processes. Proteoglycan plaques also occurred on the upper cell surface where they often appeared as a meshwork of spots and fibrils organized in complex aster-like structures (Fig. 12*a*). Such proteoglycan plaques were visible within one day of plating embryonic muscle cells, and increased in both number and size as the cultures aged (over

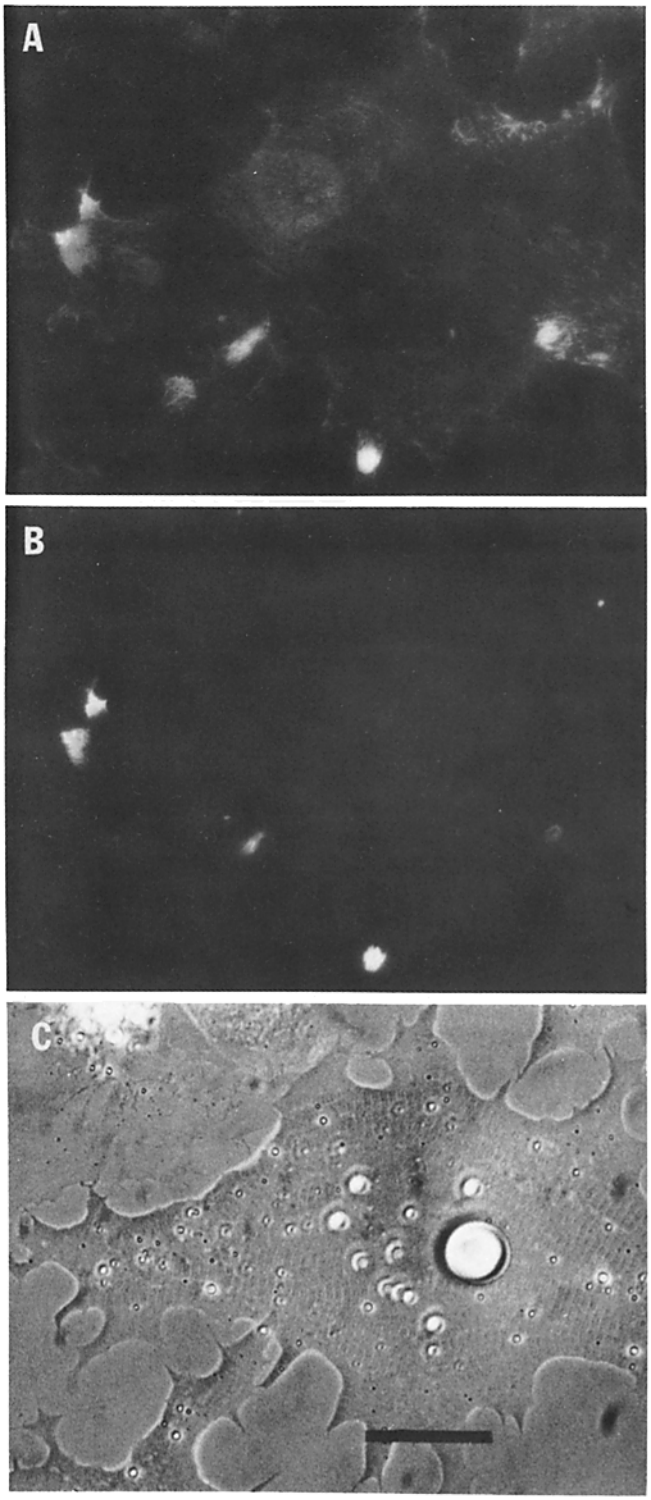

FIGURE 11 Coordinate organization of basal lamina proteoglycan and ACh receptors on a living embryonic *Xenopus* muscle cell developing in a nerve-free culture. The cell was stained with FITC-labeled monoclonal antibody (2AC2) and TRITC-labeled αBGT. The proteoglycan stain (*A*) is organized into a diffuse background separating several discrete intensely stained plaques, here viewed on the flat surface facing the collagen substratum. Many such plaques also show dense accumulations of AChR (*B*). In fact, all AChR clusters are associated with corresponding regions of dense proteoglycan staining. Bar, 30 μm. × 550.

about a week at 22°C). Older cells in culture showed a higher diffuse background of stain over their entire surface, often with a corresponding increase in the number of small plaques and fibrils.

This complex organization of cell surface proteoglycan did not seem to be an artifact of antibody labeling. It could be inhibited by previous exposure to unlabeled antibody, appeared similar whether staining was carried out with directly labeled monoclonal antibody or indirectly using fluorescent goat anti-mouse IgG, and was independent of formaldehyde fixation (data not shown).

Comparison of Proteoglycan and AChR Organization

When muscle cultures were stained with FITC-labeled antibody and counterstained with TRITC-αBGT it was possible to directly compare the organization of basal lamina proteoglycan with that of plasma membrane AChR on living cells. Such experiments revealed extensive homology in the distribution of proteoglycan-containing plaques and AChR clusters (Figs. 11 and 12). Essentially all AChR clusters were found to be associated with adjacent plaques of basal lamina proteoglycan. In fact, the congruence in the surface organization of the separate markers within such chemically specialized regions was remarkable (Fig. 12). This was true of structures on both lower and upper surfaces of the muscle cell. This latter observation is of some significance since the upper cell surface is exposed only to the culture medium and its organization is thus unlikely to have been influenced by either adhesive interaction with the substrate, or some unseen local chemical or physical irregularity of its collagen coating. As was the case at the adult neuromuscular junction (see above), the congruence between AChR and proteoglycan organization was not absolute. Proteoglycan plaques commonly extended beyond the visible borders of their AChR cluster (Fig. 12) and many proteoglycan plaques were not associated with any detectable AChR staining (Fig. 11). It is nevertheless unlikely that such a close homology in the surface organization of AChR and proteoglycan could arise fortuitously.

Proteoglycan Organization at the Embryonic Neuromuscular Junction

When dissociated *Xenopus* neural tube cells are added to aneural muscle cultures they establish functional neuromuscular junctions within 1–2 d (13, 59, 60). Over this period mobile AChR aggregate into a number of discrete clusters along the path of nerve-muscle contact (12, 13). In fact, the existence of AChR clusters along paths of nerve-muscle contact is almost invariably associated with the establishment of functional cholinergic neuromuscular junctions in this preparation (60). In our study we exploited this characteristic to examine the organization of basal lamina proteoglycan at developing neuromuscular junctions, and to compare this organization with the structure of the nerve-induced AChR clusters at the site of innervation. Examples of such stained cells are shown in Fig. 13.

As was the case in aneural muscle cultures, the AChR clusters (visualized by TRITC-αBGT staining) at developing neuromuscular junctions were all associated with morphologically congruent plaques stained with anti-proteoglycan antibody (2AC2). This was the case both for the extensive AChR

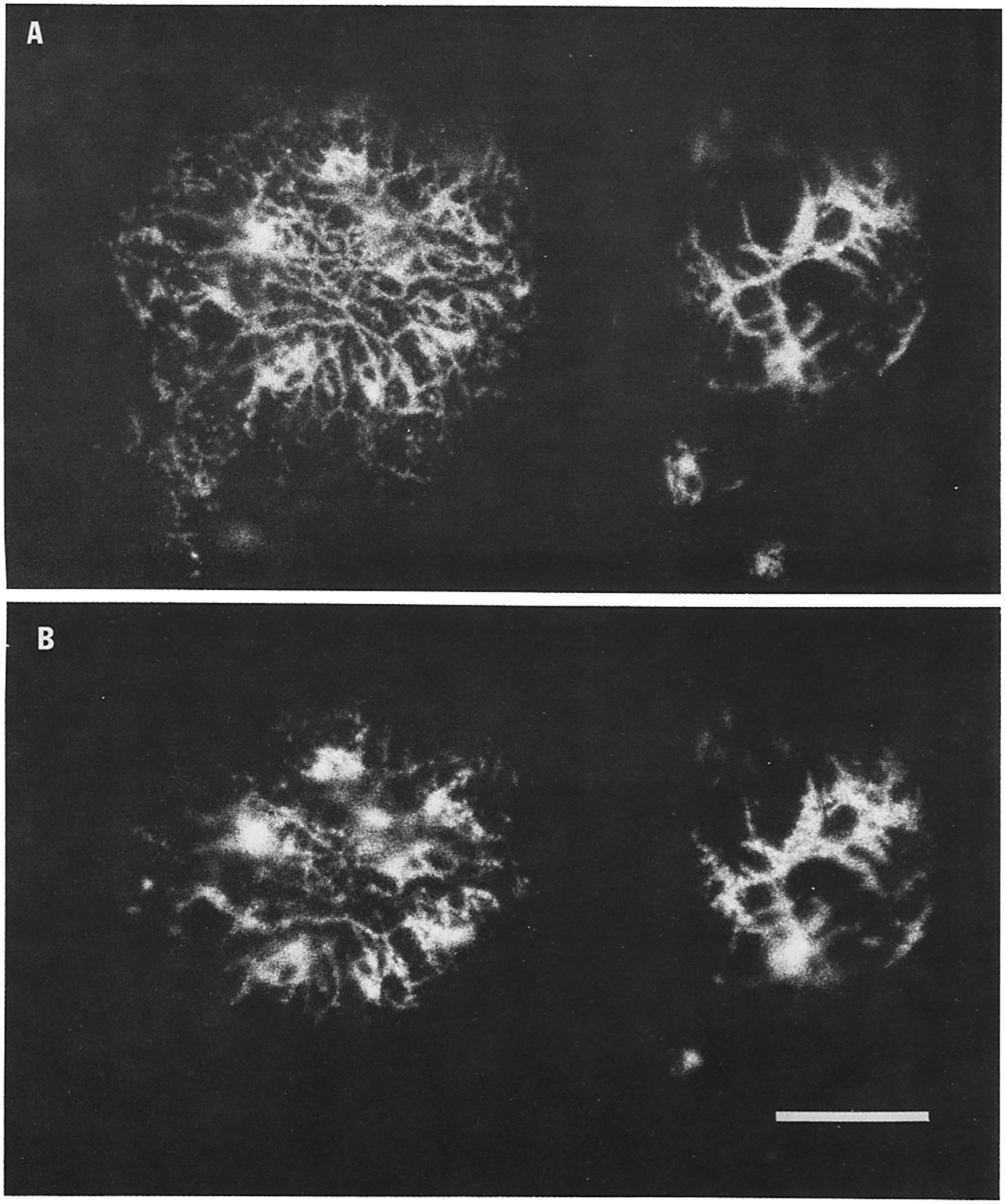

FIGURE 12 Congruence of proteoglycan and receptor organization within specialized regions of the muscle surface. A higher magnification of the upper surface of an aneural muscle cell stained as in Fig. 11, except that antibody staining intensity (*A*) was augmented by a further treatment with FITC-labeled goat anti-mouse antibody. Note that, even within such specialized regions of the muscle cell surface, all sites of clustered AChR (*B*) are associated with homologous sites of proteoglycan specialization (*A*), but not the reverse. Bar 10 μm. × 2,600.

bands at relatively mature junctions (Fig. 13, *b*, *d*, and *f*) and for the smaller AChR clusters present at earlier developmental stages (Fig. 13, *a*, *c*, and *e*). As at adult junctions the proteoglycan plaques stained with FITC-labeled antibody sometimes extended beyond the AChR clusters visualized by TRITC-αBGT, and often projected laterally several micrometers away from the path of nerve contact visible in phase-contrast optics.

Since these AChR clusters have been shown to form *de novo* as a consequence of nerve-muscle interaction (12, 13) it is reasonable to suppose that their associated basal lamina

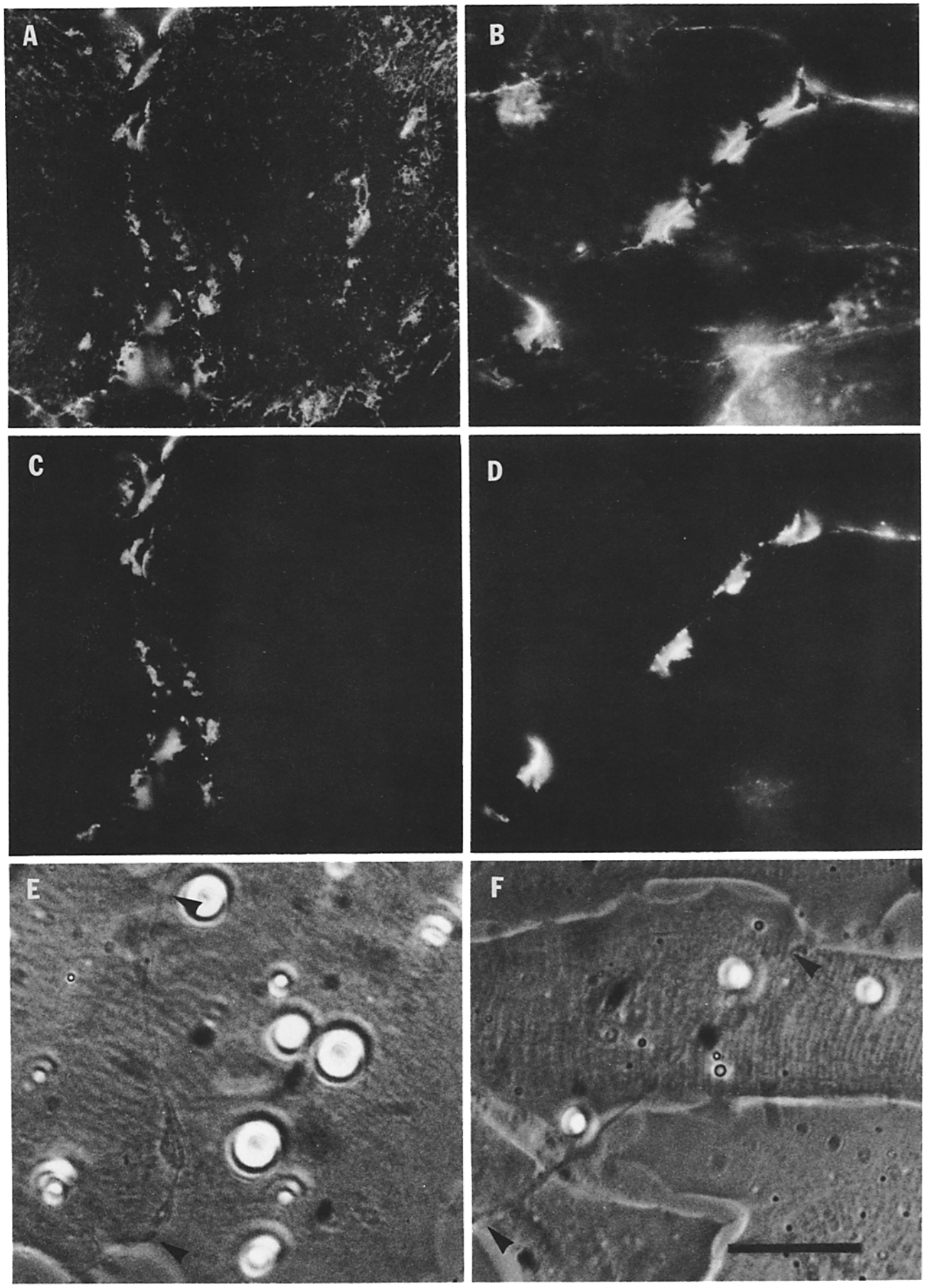
A
B
C
D
E
F

proteoglycan plaques are also under neural regulation during synaptogenesis.

DISCUSSION

In this study we used hybridoma techniques to identify a novel postsynaptic element of the chemically specialized neuromuscular junction. Quantitative electron microscope autoradiography and morphometry demonstrated that the junctional basal lamina is enriched at least fivefold, relative to adjacent morphologically similar regions of extrajunctional lamina, in a large sulfated proteoglycan. Based upon its sensitivity to partially purified *Flavobacterium* heparinase, and insensitivity to *Proteus* chondroitinase ABC, it is reasonable to conclude that this antigen belongs to the class of heparan sulfate proteoglycans, which is known to be present in basement membranes (52–55). Because of its large size, and the presence of sulfated glycosaminoglycan side chains, our estimate of a 430,000–580,000 mol wt should be viewed as an approximation. Ignoring errors implicit in such analysis, the proteoglycan appears to consist of a large ($M_r \simeq 400{,}000$) core protein with a further 100,000–200,000 mol wt presumably divided among several glycosaminoglycan side chains. Interestingly, the electrophoretic behavior of this proteoglycan is remarkably sensitive to reduction, indicating that it has a tertiary structure maintained in part by disulfide bridges within the core protein.

This basal lamina proteoglycan shows a complex surface organization that, in both adult and embryonic muscle, is closely correlated with dense accumulations of AChR in the adjacent plasmalemma. Indeed, in a parallel study of extracellular matrix elaboration in avian myogenic cultures we found that a similar heparan sulfate proteoglycan shows a higher correlation in surface organization with AChR clusters than several other extracellular matrix elements, including the basal lamina glycoprotein laminin (E. K. Bayne, M. J. Anderson and D. M. Fambrough, manuscript in preparation).

It is already well established that the neuromuscular junction is highly specialized at all structural levels. However, much of this specialization has appeared directly related to its synaptic function. Thus the presence of junctional accumulations of AChR (1, 23), AChE (2–5) or the unique antigens of synaptic vesicles (11) can all be viewed in terms of their physiological roles in the activity of the synapse. In contrast, a dense junctional specialization of a basal lamina proteoglycan is less readily interpretable in direct functional terms, and is thus more likely to be involved in maintaining the structural integrity of the synapse. The attribution of structural roles to proteoglycans is commonplace (45, 47), and has developed historically from pioneering studies that have analyzed the abundant chondroitin sulfate proteoglycans of hyaline cartilage (45, 47, 48). However, there are few compelling reasons to presume that proteoglycans are limited to analogous structural roles in other tissues.

While the present study has emphasized the synaptic localization of this proteoglycan, it is obvious that such a widely distributed component of basement membranes is not uniquely related to synaptic function. Other laboratories, systematically analyzing the chemical composition of basement membrane-like structures synthesized by murine connective tissue cell lines, have isolated and characterized heparan sulfate proteoglycan fractions whose properties appear reminiscent of the frog proteoglycan examined in this study (46, 55). In fact, heparan sulfate proteoglycans appear to be a widely distributed class of proteins generally found in association with basement membranes and cell surfaces (52–55, 62–66). Their conspicuous size dispersity and the highly anionic character of their glycosaminoglycan side chains make individual proteoglycans difficult to purify to homogeneity by conventional physical techniques. It thus remains unclear whether basal laminae, for example, contain one or many different gene products with heparan sulfate side chains. The capacity of monoclonal antibodies to distinguish both common antigenic sites, and subtle variations in molecular structure among such related macromolecular species, should eventually permit a more systematic identification and characterization of proteoglycans than has been possible up to now.

In spite of such methodological problems, a number of reports have analyzed the chemical composition, tissue distribution, and metabolism of proteoglycans, most commonly in terms of their glycosaminoglycan side chains (for a review, see reference 49). Such studies have suggested a number of potential roles for proteoglycans which could be mediated by the properties of their highly charged glycosaminoglycans. Most interesting are observations that have suggested that proteoglycans are involved in the adhesive interactions which bind cells to one another and to extracellular matrix. High affinity binding of heparin-like glycosaminoglycans (such as heparan sulfate) has been noted to both fibronectin (67–70) and laminin (71), glycoproteins of extracellular matrix that appear to contribute to cell adhesion. It should also be noted that some forms of heparan sulfate also show a strong tendency to self-associate (72), and that many of these interactions in vivo should lead to the cross-linking of adjacent multivalent molecules into extensive supramolecular structures (73).

The concentration of a basal lamina proteoglycan at the neuromuscular junction, as well as its association with myotendonous junctions and clusters of extrajunctional AChR in cultured aneural muscle, suggests that this proteoglycan could play related roles in nerve-muscle adhesion, and in the regulation of molecular organization at the synapse. Nerve and muscle cells are bound to one another at the neuromuscular junction, and this adhesion is disrupted by proteolytic removal of the basal lamina (74, 75). The dense junctional accumulation of this basal lamina proteoglycan might thus contribute toward the anchoring of adjacent synaptic components into a localized, chemically specialized region of the

FIGURE 13 Coordinate distribution of proteoglycan and AChR at neuromuscular junctions developing in cell culture. Embryonic *Xenopus* muscle cells were innervated by developing motor neurites in cell culture and then stained as in Fig. 12. Dense proteoglycan accumulations (*a* and *b*) were found associated with all the developing clusters of junctional AChR (*c* and *d*) found along paths of nerve-muscle contact (arrows) visible in phase-contrast (*e* and *f*). On such innervated cells extrajunctional proteoglycan deposits remained abundant (*a* and *b*) even in the absence of extrajunctional AChR clusters. Bar 20 μm. × 1,200.

cell. This possibility is also consistent with observations that the collagenous synaptic form of AChE binds with high affinity to basal lamina heparan sulfate proteoglycans extracted from the murine EHS sarcoma (76) and can be precipitated by sulfated proteoglycans extracted from extracellular matrix of the electroplax (77). The presence of heparan sulfate proteoglycan at AChR clusters on developing muscle cells may thus help to explain the observations that such clusters appear also to be associated with regions of high AChE activity (78) and deposits of amorphous extracellular material (79).

While our experiments suggest there may be an obligatory association of AChR clusters with surface accumulations of a basal lamina proteoglycan, the reverse is certainly not the case. It is thus not adequate to explain the AChR organization on muscle cells simply by postulating a direct interaction between AChR and proteoglycan molecules. Earlier studies have also shown that AChR clusters are associated with regions of cytoskeletal specialization, both at the neuromuscular junction (6–8) and on aneural muscle cells in culture (80). Since these regions appear also to be sites of adhesion for the muscle cell (74, 75, 80), it is most likely that the clustering of AChR is related to the assembly of a transmembrane-complex of structural proteins, including basal lamina proteoglycan, at adhesion sites. The reasons why AChR dissociate from one such specialized site and aggregate at another during synaptogenesis (12–14) still remain an interesting puzzle.

We are grateful to Ms. J. Lippincott-Schwartz and to Drs. V. Hascall, N. Lipsky, K. Muller, and R. Pagano for numerous useful suggestions. We also thank Drs. G. Martin and J. Hassel for advice and for a sample of heparinase (prepared by Dr. A. Linker). We are indebted to Ms. S. Satchell for the preparation of the manuscript and to Mrs. D. Somerville for technical assistance. Mr. R. Grill also provided valuable assistance in preparing several illustrations.

This work was supported by grants from the Muscular Dystrophy Association of America and the National Institutes of Health to D. M. Fambrough.

Received for publication 28 March 1983, and in revised form 27 June 1983.

REFERENCES

1. Fertuck, H. C., and M. M. Salpeter. 1976. Quantitation of junctional acetylcholine receptors by electron microscope autoradiography after ^{125}I-α-bungarotoxin binding at mouse neuromuscular junctions. *J. Cell Biol.* 69:144–158.
2. Couteaux, R. 1955. Localization of cholinesterases at neuromuscular junctions. *Int. Rev. Cytol.* 4:335–375.
3. Fambrough, D. M., A. G. Engel, and T. L. Rosenberry. 1982. Acetylcholinesterase of human erythrocytes and neuromuscular junctions: homologies revealed by monoclonal antibodies. *Proc. Natl. Acad. Sci. USA* 79:1078–1082.
4. Salpeter, M. M. 1967. Electron microscope radioautography as a quantitative tool in enzyme cytochemistry. I. The distribution of acetylcholinesterase at motor endplates of a vertebrate twitch muscle. *J. Cell Biol.* 32:379–389.
5. McMahan, U. J., J. R. Sanes, and L. M. Marshall. 1978. Cholinesterase is associated with the basal lamina at the neuromuscular junction. *Nature (Lond.).* 193:281–282.
6. Froehner, S. C., V. Gulbrandsen, C. Hyman, A. Y. Yeng, R. R. Neubig, and J. B. Cohen. 1981. Immunofluorescence localization at the mammalian neuromuscular junction of the M_r 43,000 protein of *Torpedo* synaptic membranes. *Proc. Natl. Acad. Sci. USA.* 78:5230–5234.
7. Hall, Z. W., B. W. Lubit, and J. H. Schwartz. 1981. Cytoplasmic actin in postsynaptic structures at the neuromuscular junction. *J. Cell Biol.* 90:789–792.
8. Burden, S. 1982. Identification of an intracellular postsynaptic antigen at the frog neuromuscular junction. *J. Cell Biol.* 94:521–530.
9. Sanes, J. R., and Z. W. Hall. 1979. Antibodies that bind specifically to synaptic sites on muscle fiber basal lamina. *J. Cell Biol.* 83:357–370.
10. Sanes, J. R., S. S. Carlson, R. Von Wedel, and R. B. Kelly. 1979. Antiserum specific for motor nerve terminals in skeletal muscle. *Nature (Lond.).* 280:403–404.
11. Hooper, J. E., S. S. Carlson, and R. B. Kelly. 1980. Antibodies to synaptic vesicles purified from murine electric organ bind a subclass of mammalian nerve terminals. *J. Cell Biol.* 87:104–113.
12. Anderson, M. J., and M. W. Cohen. 1977. Nerve-induced and spontaneous redistribution of acetylcholine receptors on cultured muscle cells. *J. Physiol. (Lond.).* 268:757–773.
13. Anderson, M. J., M. W. Cohen, and E. Zorychta. 1977. Effects of innervation on the distribution of acetylcholine receptors on cultured amphibian muscle cells. *J. Physiol. (Lond.).* 268:731–756.
14. Frank, E. L., and R. D. Fischbach. 1979. Early events in neuromuscular junction formation *in vitro*. Induction of acetylcholine receptor clusters in the postsynaptic membrane and morphology of newly formed synapses. *J. Cell Biol.* 83:143–158.
15. Lømo, T., and C. R. Slater. 1978. Control of acetylcholine sensitivity and synapse formation by muscle activity. *J. Physiol. (Lond.).* 275:391–402.
16. Sytkowski, A. J., Z. Vogel, and M. W. Nirenberg. 1973. Development of acetylcholine receptor clusters on cultured muscle cells. *Proc. Natl. Acad. Sci. USA.* 70:270–274.
17. Fischbach, G. D., and S. A. Cohen. 1973. The distribution of acetylcholine sensitivity over uninnervated and innervated muscle fibers grown in cell culture. *Dev. Biol.* 31:147–162.
18. Ko, P. K., M. J. Anderson, and M. W. Cohen. 1977. Denervated skeletal muscle fibers develop patches of high acetylcholine receptor density. *Science (Wash. DC).* 196:540–542.
19. Burden, S. J., P. B. Sargent, and U. J. McMahan. 1979. Acetylcholine receptors in regenerating muscle accumulate at original synaptic sites in the absence of nerve. *J. Cell Biol.* 82:412–425.
20. Axelrod, D., P. Ravdin, D. E. Koppel, J. Schlessinger, W. W. Webb, E. L. Elson, and T. R. Podleski. 1976. Lateral motion of fluorescently labeled acetylcholine receptors in membranes of developing muscle fibers. *Proc. Natl. Acad. Sci. USA.* 73:4594–4598.
21. Köhler, G., and C. Milstein. 1976. Derivation of specific antibody-producing tissue and tumor lines by cell fusion. *Eur. J. Immunol.* 6:511–519.
22. Kennett, R. H., K. A. Denis, A. S. Tung, and N. R. Klinman. 1978. Hybrid plasmacytoma production: fusion with adult spleen cells, monoclonal spleen fragments, neonatal spleen cells and human spleen cells. *Curr. Topics Microbiol. Immunol.* 81:77–93.
23. Anderson, M. J., and M. W. Cohen. 1974. Fluorescent staining of acetylcholine receptors in vertebrate skeletal muscle. *J. Physiol. (Lond.).* 237:385–400.
24. Laemmli, U. K., and M. Favre. 1970. Maturation of the head of bacteriophage T4. *J. Mol. Biol.* 80:575–597.
25. Bonner, W. M., and R. A. Laskey. 1974. A film detection method for tritium-labelled proteins and nucleic acids in polyacrylamide gels. *Eur. J. Biochem.* 46:83–88.
26. Laskey, R. A., and A. D. Mills. 1975. Quantitative film detection of ^{3}H and ^{14}C in polyacrylamide gels by fluorography. *Eur. J. Biochem.* 56:335–341.
27. Nieuwkoop, P. D., and J. Faber. 1956. Normal Table of *Xenopus laevis*. 2nd edition. Elsevier/North Holland, Amsterdam. 162–188.
28. Suzuki, S. 1972. Chondroitinases from *Proteus vulgarus* and *Flavobacterium heparinum*. *Methods Enzymol.* 28:911–917.
29. Hovingh, P., and A. Linker. 1970. The enzymatic degradation of heparin and heparitin sulfate. III. Purification of a heparitinase and a heparinase from Flavobacteria. *J. Biol. Chem.* 245:6170–6175.
30. Linker, A., and P. Hovingh. 1972. Heparinase and heparitinase from Flavobacteria. *Methods Enzymol.* 28:903–911.
31. Gill, P. J., J. Adler, C. K. Silbert, and J. E. Silbert. 1981. Removal of glycosaminoglycans from cultures of human skin fibroblasts. *Biochem. J.* 194:299–307.
32. Greenwood, F. C., N. M. Hunter, and J. S. Glover. 1963. The preparation of ^{131}I-labelled human growth hormone of high specific radioactivity. *Biochem. J.* 89:114–123.
33. Caro, L. G., and R. P. van Tubergen. 1962. High resolution autoradiography. *J. Cell Biol.* 15:173–188.
34. Salpeter, M. M., L. Bachman, and E. E. Salpeter. 1969. Resolution in electron microscope radioautography. *J. Cell Biol.* 41:1–20.
35. Röhde, H., G. Wick, and R. Timpl. 1979. Immunochemical characterization of the basement membrane glycoprotein laminin. *Eur. J. Biochem.* 102:195–201.
36. Krieg, T., R. Timpl, K. Alitalo, M. Kurkinen, and A. Vaheri. 1979. Type III procollagen is the major collagenous component produced by a continuous rhabdomyo-sarcoma cell lines. *FEBS (Fed. Eur. Biochem. Soc.) Lett.* 104:405–409.
37. Fessler, J. H., and L. I. Fessler. 1978. Biosynthesis of procollagen. *Annu. Rev. Biochem.* 47:129–162.
38. Bornstein, P., and H. Sage. 1980. Structurally distinct collagen types. *Annu. Rev. Biochem.* 49:957–1003.
39. Wilson, B. W., P. S. Nieberg, C. R. Walker, T. A. Linkhart, and D. M. Fry. 1973. Production and release of acetylcholinesterase by cultured chick embryo muscle. *Dev. Biol.* 33:285–299.
40. Olden, K., and K. M. Yamada. 1977. Mechanism of the decrease in the major cell surface protein of chick embryo fibroblasts after transformation. *Cell.* 11:957–969.
41. Cheng, A. E., R. Jaffe, I. L. Freeman, J. P. Vergnes, J. E. Braginski, and B. Carlin. 1979. Properties of a basement membrane-related glycoprotein synthesized in culture by a mouse embryonal carcinoma-derived cell line. *Cell.* 16:277–287.
42. Kühl, U., R. Timpl, and K. von der Mark. 1982. Synthesis of type IV collagen and laminin in cultures of skeletal muscle cells and their assembly on the surface of myotubes. *Dev. Biol.* 93:344–354.
43. Hogan, B. L. M., A. Taylor, M. Kurkinen, and J. R. Couchman. 1982. Synthesis and localization of two sulphated glycoproteins associated with basement membranes and the extracellular matrix. *J. Cell Biol.* 95:197–204.
44. Yonekura, H., K. Oguri, K. Nakazawa, S. Shimizu, Y. Nakanishi, and M. Okayama. 1982. Isolation and partial characterization of sulfated glycoproteins synthesized by corneal epithelium. *J. Biol. Chem.* 257:11166–11175.
45. Hascall, V. C. 1981. Proteoglycans: structure and function. *In* Biology of Carbohydrates. V. Ginsburg, editor. John Wiley & Sons, Inc., New York. I: 1–49.
46. Oohira, A., T. N. Wight, J. McPherson, and P. Bornstein. 1982. Biochemical and ultrastructural studies of proteoheparan sulfates synthesized by PYS-2, a basement membrane-producing cell line. *J. Cell Biol.* 92:357–467.
47. Hay, E. D. 1981. Extracellular matrix. *J. Cell Biol.* 91(3, Pt. 2):205s–223s.
48. Hascall, V. C., and S. W. Sajdera. 1970. Physical properties and polydispersity of proteoglycan from bovine nasal cartilage. *J. Biol. Chem.* 245:4920–4930.
49. Lindahl, U., and M. Höök. 1978. Glycosaminoglycans and their binding to biological macromolecules. *Annu. Rev. Biochem.* 47:385–417.
50. Hay, E. D., and S. Meier. 1974. Glycosaminoglycan synthesis by embryonic inductors: neural tube, notochord and lens. *J. Cell Biol.* 62:889–898.
51. Trelstad, R. L., K. Hayashi, and B. P. Toole. 1974. Epithelial collagens and glycosaminoglycans in the embryonic cornea. Macromolecular order and morphogenesis in the basement membrane. *J. Cell Biol.* 62:815–830.
52. Cohn, R. H., S. D. Banerjee, and M. R. Bernfield. 1977. Basal lamina of embryonic salivary epithelia. Nature of glycosaminoglycan and organization of extracellular materials. *J. Cell Biol.* 73:464–478.

53. Kanwar, Y. S., and M. G. Farquhar. 1979. Presence of heparan sulfate in the glomeralar basement membrane. *Proc. Natl. Acad. Sci. USA.* 76:1303–1307.
54. Kanwar, Y. S., and M. G. Farquhar. 1979. Anionic sites in the glomerular basement membrane. In vivo and in vitro localization to the lamina rara by cationic probes. *J. Cell Biol.* 81:137–153.
55. Hassell, J., P. G. Robey, H. J. Barrach, J. Wilczek, S. I. Rennard, and G. R. Martin. 1980. Isolation of heparan sulfate containing proteoglycan from basement membrane. *Proc. Natl. Acad. Sci. USA.* 77:4494–4498.
56. Kosher, R. A., and R. L. Searls. 1973. Sulfated mucopolysaccharide synthesis during the development of *Rana pipiens*. *Dev. Biol.* 32:50–68.
57. Nahazawa, K., and S. Suzuki. 1975. Purification of keratan sulfate-endogalactosidase and its action on keratan sulfates of different origin. *J. Biol. Chem.* 250:912–917.
58. Wernig, A., M. Pecot-Dechavassine, and H. Stover. 1980. Sprouting and regression of the nerve at the frog neuromuscular junction in normal conditions and after prolonged paralysis with curare. *J. Neurocytol.* 9:277–303.
59. Anderson, M. J., Y. Kidokoro, and R. Gruener. 1979. Correlation between acetylcholine receptor localization and spontaneous synaptic potentials in cultures of nerve and muscle. *Brain. Res.* 166:185–190.
60. Kidokoro, Y., M. J. Anderson, and R. Gruener. 1980. Changes in synaptic potential properties during acetylcholine receptor accumulation and neurospecific interactions in *Xenopus* nerve-muscle cell culture. *Dev. Biol.* 78:464–483.
61. Weldon, P. R., and M. W. Cohen. 1979. Development of synaptic ultrastructure at neuromuscular contacts in an amphibian cell culture system. *J. Neurocytol.* 8:239–259.
62. Kraemer, P. M. 1971. Heparan sulfates of cultured cells. I. Membrane associated and cell-sap species in Chinese hamster cells. *Biochemistry.* 10:1437–1445.
63. Oldberg, A., M. Höök, B. Obrink, H. Pertoft, and K. Rubin. 1977. Structure and metabolism of rat liver heparan sulphate. *Biochem. J.* 164:75–81.
64. Hedman, K., M. Kurkinen, K. Alitalo, A. Vaheri, S. Johansson, and M. Höök. 1979. Isolation of the pericellular matrix of human fibroblast cultures. *J. Cell Biol.* 81:83–91.
65. Oldberg, A., L. Kjellen, and M. Höök. 1979. Cell surface heparan sulfate. Isolation and characterization of a proteoglycan from rat liver membranes. *J. Biol. Chem.* 254:8505–8510.
66. Rollins, B. J., and L. A. Culp. 1979. Glycosaminoglycans in the substrate adhesion sites of normal and virus-transformed murine cells. *Biochemistry.* 18:141–148.
67. Stathakis, N. E., and M. L. Mosesson. 1977. Interactions among heparin, cold-insoluble globulin, and fibrinogen in formation of the heparin-precipitable fraction of plasma. *J. Clin. Invest.* 60:855–865.
68. Jilek, F., and H. Hormann. 1979. Fibronectin (cold-insoluble globulin). IV. Influence of heparin and hyaluronic acid on the binding of native collagen. *Hoppe-Seyler's Z. Physiol. Chem.* 360:597–603.
69. Ruoslahti, E., and E. Engvall. 1980. Complexing of fibronectin glycosaminoglycans and collagen. *Biochem. Biophys. Acta.* 631:350–358.
70. Yamada, K. M., D. W. Kennedy, K. Kimata, and R. M. Pratt. 1980. Characterization of fibronectin interactions with glycoaminoglycans and identification of active proteolytic fragments. *J. Biol. Chem.* 255:6055–6063.
71. Sakashita, S., E. Engvall, and E. Ruoslahti. 1980. Basement membrane glycoprotein laminin binds to heparin. *FEBS (Fed. Eur. Biochem. Soc.) Lett.* 116:243–246.
72. Fransson, L. A., B. Hausmark, and J. K. Sheehan. 1981. Self-association of heparan sulfate. Demonstration of binding by affinity chromatography of free chains on heparan sulfate-substituted agarose gels. *J. Biol. Chem.* 256:13039–13043.
73. Hayman, E. G., Å. Oldberg, G. R. Martin, and E. Ruoslahti. 1982. Condistribution of heparan sulfate proteoglycan, laminin and fibronectin in the extracellular matrix of normal rat kidney cells and their coordinate absence in transformed cells. *J. Cell Biol.* 94:28–35.
74. Hall, Z. W., and R. B. Kelly. 1971. Enzymatic detachment of endplate acetylcholinesterase from muscle. *Nature (New Biol.).* 232:62–64.
75. Betz, W., and B. Sackmann. 1973. Effects of proteolytic enzymes on function and structure of frog neuromuscular junctions. *J. Physiol. (Lond.).* 230:673–688.
76. Vigny, M., G. R. Martin, and G. R. Grotendorst. 1983. Interactions of asymmetric forms of acetylcholinesterase with basement membrane components. *J. Biol. Chem.* 258:8794–8798.
77. Bon, S., J. Cartaud, and J. Massoulie. 1978. The dependance of acetylcholinesterase aggregation at low anionic strength upon a polyanionic component. *Eur. J. Biochem.* 85:1–14.
78. Moody-Corbett, F., and M. W. Cohen. 1981. Localization of cholinesterase at sites of high acetylcholine receptor density on embryonic amphibian muscle cells cultured without nerve. *J. Neurosci.* 1:596–605.
79. Burrage, T. G., and T. L. Lentz. 1981. Ultrastructural characterization of surface specializations containing high density acetylcholine receptors on embryonic chick myotubes *in vivo* and *in vitro*. *Dev. Biol.* 85:267–286
80. Bloch, R. J., and B. Geiger. 1980. The localization of acetylcholine receptor clusters in areas of cell-substrate contact in cultures of rat myotubes. *Cell.* 21:25–35.